J Mater Sci (2010) 45:1947–1954
DOI 10.1007/s10853-009-4186-0

Synthesis of polypyrrole film by pulse galvanostatic method and its application as supercapacitor electrode materials

Jing Zhang · Ling-Bin Kong · Heng Li · Yong-Chun Luo · Long Kang

Received: 5 November 2009 / Accepted: 28 December 2009 / Published online: 12 January 2010

Abstract Polypyrrole (PPy) film-coated stainless steel electrodes were prepared from aqueous solution containing 0.5 M p-toluene sulphonic acid and 0.1 M pyrrole using pulse galvanostatic method (PGM) and galvanostatic method (GM). The morphology was characterized by scanning electron microscopy. The electrochemical properties of PPy films were investigated with cyclic voltammetry, charge–discharge tests, and ac impedance spectroscopy. The results showed that the PGM-PPy films exhibited higher specific capacitance, better high-rate discharge ability and lower resistance, and were more promising for applications in supercapacitor than GM-PPy films. The specific capacitance (SC) of PGM-PPy films was 403 F g^{-1} in 1 M H_2SO_4 electrolyte and 281 F g^{-1} in 1 M $NaNO_3$ electrolyte.

Introduction

Electrically conducting polymers (ECPs) have attracted considerable attention because of their unusual electronic properties [1–3]. Of all known ECPs, polypyrrole (PPy) is by far the most extensively studied on account of the monomer (pyrrole) being easily oxidized, water soluble, and commercial applications, including secondary batteries [4, 5], fuel cells [6], supercapacitors [7, 8], sensors [9, 10], anhydrous electrorheological fluids [11], and corrosion protection [12]. More recently, improvements in properties of PPy have been achieved using composites with multi-wall [13, 14] and single-wall [15, 16] carbon nanotubes embedded in the PPy but the cost of composites has also increased accordingly. Hence, looking for new synthesis method to enhance the PPy electrical conductivity and increase the hydrophilicity of the polymer structure for small chain size. PPy can be prepared either chemically or electrochemically. Chemical methods can control morphology of PPy forming nanostructures [17–19], but they require relatively larger amounts of surfactants, which are rather tedious to recycle after polymerization. Moreover, it is difficult to attach nanosized polypyrrole onto a substrate without involving large contact resistance. Therefore, the nanosized polypyrrole synthesized by such methods is not suitable for electrochemical applications. Electrochemical polymerization of PPy onto a substrate directly may be the best way to solve the aforementioned problem. Electrochemical techniques including potentiostatic method (PM) [20], galvanostatic method (GM) [21], and cyclic voltammetric method (CVM) [22] are widely employed in electropolymerization of pyrrole. Modified potentiostatic and galvanostatic methods are reported by some researchers as well. Pulse potentiostatic method (PPM) and pulse galvanostatic method (PGM) for the electrochemical deposition of conducting polymers films have been investigated by Schuhmann et al. [23]. Tsakova and Milchev [24], who have applied PPM to the electrodeposition of PANI films, found stronger activation of growth of PANI prepared by PPM in comparison with that prepared by Kuang et al.

J. Zhang · L.-B. Kong (✉) · H. Li
State Key Laboratory of Gansu Advanced Non-ferrous Metal Materials, Lanzhou University of Technology, 730050 Lanzhou, People's Republic of China
e-mail: konglb@lut.cn

Y.-C. Luo · L. Kang
Key Laboratory of Non-ferrous Metal Alloys and Processing of Ministry of Education, Lanzhou University of Technology, 730050 Lanzhou, People's Republic of China

[25, 26] used both PPM and PGM to prepare PANI with a nano-fibular structure. Compared with conventional GM, PGM is a modified galvanostatic polarization method, which may supply instantaneously high over-potential regardless of relatively smaller mean current. The discontinuous current can eliminate the concentration polarization at the electrode/solution interface for enough supplement of reactant. Recently, Sharma et al. [27] reported that the chain size and defects of PPy film could be controlled by applying ultra short on time current pulse for polymerization.

It has already been confirmed that conducting polymer films prepared by PGM yield good electroactivity and uniform morphology. However, these researches are focused on the effects of preparation conditions on the morphology and the electroactivity of the conducting polymer films and little attention has been drawn to the supercapacitive behavior of PGM-conducting polymer films. As known to all, because of the possible presence of benzidine moieties in the polyaniline backbone, which might yield toxic (carcinogenic) products upon degradation, the research in PANI chemistry have been limited by numerous industrial and academic groups [28]. In contrast, the PPy family is possibly more environmentally "friendly" systems and yields higher electrical conductivity, which have attracted more considerable attention in electrochemical supercapacitor application than that of PANI [29]. Therefore, the study here is aimed to investigate PGM-PPy films electropolymerized on SS substrate as supercapacitor electrodes, especially the electrochemical properties of the PGM-PPy films. Compared with GM-PPy films, the process of PGM with short t_{on} (10 ms) and longer t_{off} (100 ms) has resulted in a smooth, uniform, and small particle size of PPy film. The PGM-PPy films are formed to possess high specific capacitance (SC), good power characteristic, and small magnitude of equivalent series resistance (ESR), and are promising for applications in supercapacitor. The highest SC value of 403 F g^{-1} is obtained for a PGM-PPy film with 40 s "current on" time. In particular, the neutral electrolyte used for PGM-PPy films and the electrochemical properties has been investigated as well.

Experimental

Materials

Pyrrole was vacuum-distilled at 60 °C before being used, and then was stored at −10 °C in a nitrogen atmosphere. P-toluene sulfonate acid (TOS) was used as a surfactant and supporting salt for all the electrochemical polymerizations. Other chemicals used were of analytical grade. All solutions were prepared by double-distilled water.

Electrode preparation and characterization

An electrolyte solution of 0.5 M TOS + 0.1 M pyrrole was used for polymerization. The electrochemical synthesis of PPy films was carried out in a three-compartment electrochemical cell. A platinum sheet served as the auxiliary electrode, and a saturated calomel electrode (SCE) was used as the reference electrode. SS (type 304, 0.5 mm thick) foils were used as working electrode. Before being used, SS foils were polished with successive grades of emery to a mirror surface, and were then washed with double-distilled water in an ultrasonic bath for 15 min.

The PPy films were prepared by two methods: (i) pulse galvanostatic method (PGM) and (ii) galvanostatic method (GM) (hereinafter, denoted as PGM-PPy film and GM-PPy film, respectively). The scheme of PGM is shown in Fig. 1. i_a is the anodic a peak current of pulse; t_{off} and t_{on} are the "off" pulse off on period and "on" pulse period, respectively. The pulse procedure used for PGM-PPy film is illustrated as follows: polymerization was carried out at constant current density pulses for a period of time. Pulse on time (t_{on}) was 0.01 s and pulse off time (t_{off}) was chosen as constant 0.1 s. No current was applied during off period. Total number of on pulses was set to complete a total "current on" time of 40, 60, 90, and 120 s. For the purpose of comparison, we carried out polymerization process by GM with constant current density from 40 to 120 s.

After electropolymerization, the polymer film coating SS electrode was transferred into another electrochemical cell and was cycled between −0.4 and 0.6 V in 1 M H_2SO_4 electrolyte and 1 M $NaNO_3$ electrolyte, respectively. Cyclic voltammogram (CV) was recorded after obtaining a stable CV pattern with minimal changes in peak potential and current. All experiments were conducted under N_2 atmosphere.

The mass of pristine PPy films were determined using the electronic microbalance (BP211D, Sartorius, $d = 0.01$/0.1 mg). The morphologies of the PPy films were examined by a field emission scanning electron microscope

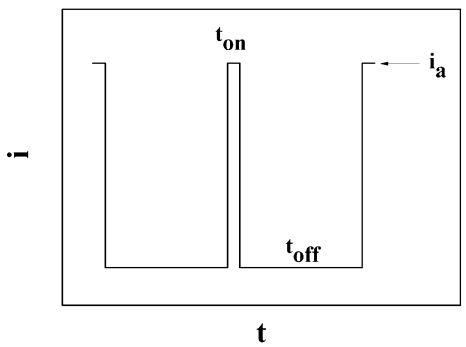

Fig. 1 A schematic representation of PGM

(JSM-6701F, JEOL). The film thickness was measured using a surface profilometer (Dektak150).

Electrochemical tests

All electrochemical experiments were performed by a CHI660C electrochemical workstation (Shanghai Chenhua Instrument Factory, China) in a glass cell with working electrode, a platinum sheet counter electrode, and a standard SCE.

The electrochemical tests were carried in 1 M H_2SO_4 and 1 M $NaNO_3$ aqueous solution for the purpose to compare capacitive behavior of PPy film. CV scans were recorded from −0.4 to 0.6 V at 5 mV s^{-1}, and charge–discharge cycle tests were carried out at different constant current densities, with cutoff voltages of −0.4 to 0.6 V. EIS measurements for the PPy film electrodes were performed in an ac frequency range from 100,000 to 0.01 Hz with an excitation signal of 5 mV. All electrochemical experiments were carried out at 20 ± 1 °C.

Results and discussion

Microstructure of the PPy films

In our study, we prepared PPy films at equivalent total charge by two different methods: PGM and GM. Under SEM, both the PGM-PPy film and GM-PPy film presented uniform microstructures. In Fig. 2a, the PGM-PPy film whose horn-like structures with particle size ranging from 1 to 4 μm is obviously short in comparison to GM-PPy film (Fig. 2b). A uniform morphology of PGM-PPy film shown in Fig. 1a is desirable because it enables a material with high diffusivity for the electrolyte ions to achieve fast charge/discharge rates. However, the GM-PPy film presented in Fig. 2b shows a disorder surface with large particle size. Such a structure is expected to result in kinetically inferior electrochemical performance in comparison with PGM-PPy film. Hence, it can be concluded that the smaller particle size formed in PGM-PPy film is due to the process of polymerization with short t_{on} (10 ms) and longer t_{off} (100 ms). During t_{on}, the polymer chain has nucleated over the SS-substrate surface only for a very short period, and then followed by t_{off}. The growth on the initial sites of the electrode is frustrated during the longer t_{off}. Hence, the growth on the fresh sites of the electrode is more probable, thus forming a large number of equivalent nucleation and growth sites [27, 30]. As we expected, the application of ultra short pulse on time for polymerization has a definite effect on the polymer structure. The PGM-PPy film exhibited uniform microstructures with small particle size, which were the ideal structure for supercapacitor electrode due to their improved hydrophilic character.

Electrochemical response of PPy films

For the purpose of studying the relationship between polymerization time and specific capacitance (SC) of PPy films, polymerization was carried out at constant current density (4 mA cm^{-2}) in all the growth experiments by the total "current on" time 40, 60, 90, and 120 s, respectively. The SC of PPy film electrodes in both 1 M H_2SO_4 and 1 M $NaNO_3$ electrolyte can be obtained from discharge curves (as shown in Fig. 3) by the following relationship, i.e., $C_d = I\Delta t/\Delta E$m. Here, I is the discharge current, Δt is the discharge time corresponding to the voltage difference (ΔE), and m is the active electrode mass. The polymerization time, mass, and thickness of films corresponding to the SC are given in Table 1. It is noted that there is a decrease in capacitance with further growth time of PPy films for both polymerization method. It is in consistent with the studies reported in the literature where a similar relationship between capacitance with thickness of PANI as reported earlier [31]. The electrochemical properties of PPy film are strongly influenced by the morphology and thickness. According to the results in Table 1, thinner PPy films can present better charge carrier mobility [32], which permit higher SC. With the same total "current on" time of

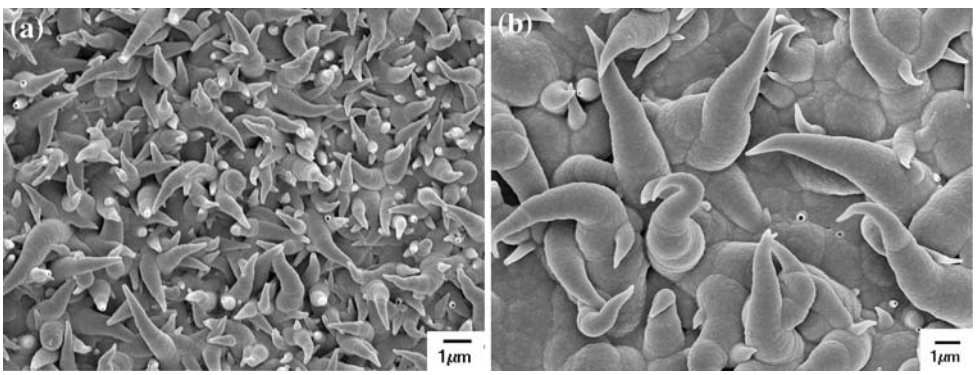

Fig. 2 SEM images of the PGM-PPy film (**a**) and GM-PPy film (**b**). The total "current on" time of PPy film is 90 s

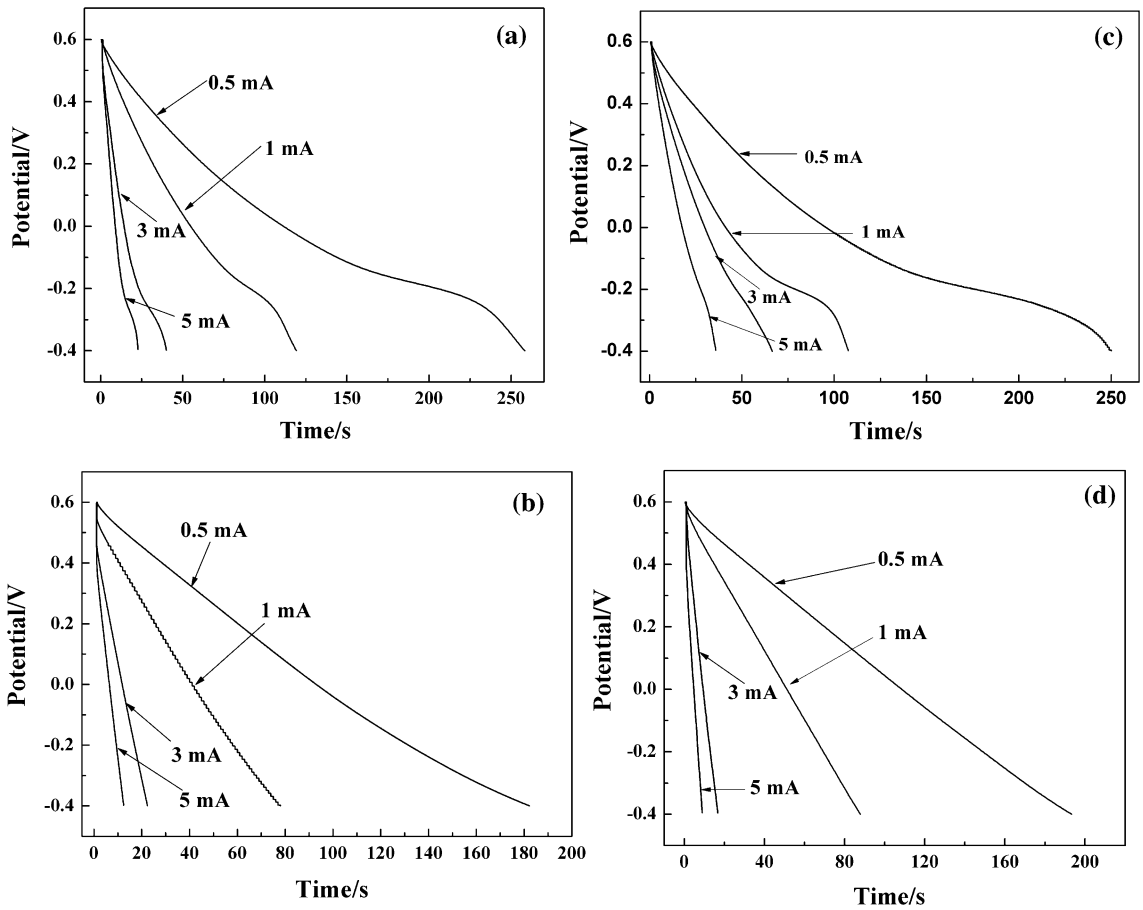

Fig. 3 Galvanostatic discharge curves of the PGM-PPy films (**a** and **b**) and GM-PPy films (**c** and **d**) at different current density. Curves (**a** and **c**) measured in 1 M H_2SO_4 electrolyte and curves (**b** and **d**) in 1 M $NaNO_3$ electrolyte. The total "current on" time of PPy film is 40 s

polymerization process, the roughness of PGM-PPy films is significantly smaller than that of GM-PPy films, which can be attributed to the limited thickness and the smaller grain size of the former. Thus, the PGM-PPy films present a favorable structural feature, for its reduced grain size and improved interchain conduction owning to a more homogeneous deposition at initial stages. In Table 1, it can be seen that for PGM-PPy film (0.8 μm) the maximum capacitance of 403 F g^{-1} was obtained with 40 s "current on" time. For the same polymerization time, the SC of PGM-PPy films were higher than GM-PPy films. Compared with GM-PPy films, the capacitance properties of PGM-PPy films were better, which was due to the pulsed process of polymerization. We can see from Fig. 2, when the current density increased from 0.5 to 5 mA cm^{-2}, the SC for PGM-PPy film is from 403 to 360 F g^{-1}, which are higher than those for GM-PPy film (from 251 to 175 F g^{-1}). Based on the above analysis, the PGM-PPy film was more available for supercapacitor electrode.

In order to compare the power properties between PGM-PPy film and GM-PPy film, the high-rate discharge ability (A) of the electrode was also employed. The A can be obtained using Eq. 1:

$$A(\%) = C_d/C_{0.5}100\% \quad (1)$$

where C_d and $C_{0.5}$ are the discharge capacity of electrodes at a certain current density and 0.5 mA cm^{-2}, respectively. Figure 4 shows the relationship between the high-rate discharge ability and the discharge current density. It was clear from Fig. 3 that the SC decreased with increasing current density due to the internal resistance of the electrode. The PGM-PPy film electrode exhibited better high-rate discharge ability when compared with GM-PPy film electrode. When the current density increased from 1 to 10 mA cm^{-2}, it only lost 10% of the initial SC even in the charge–discharge current density up to 10 mA cm^{-2}. Thus, it can be deduced that the power characteristic of this electrode was improved in the process of PGM polymerization.

Figure 5 shows the CV curves of PGM-PPy film and GM-PPy film in 1 M H_2SO_4 solution with 5 mV s^{-1} scanning rate. Although the CV shapes of both the PPy

Table 1 The SC of PPy films with different polymerization time

Polymerization method	Total "current on" time (s)	Mass of the material (mg cm^{-2})	Thickness of the PPy films (μm)	Specific capacitance (F g^{-1})	
				1 M H_2SO_4 electrolyte	1 M $NaNO_3$ electrolyte
PGM	40	0.32	0.8	403	281
	60	0.48	1.4	384	259
	90	0.86	1.6	324	221
	120	1.12	2.0	303	170
GM	40	0.5	1.7	251	193
	60	0.75	2.3	217	181
	90	0.9	2.5	185	169
	120	1.3	3.0	156	102

The current density is 0.5 mA cm^{-2}

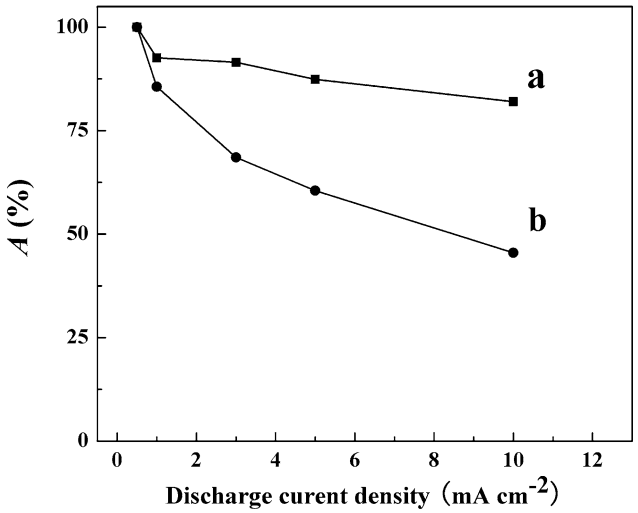

Fig. 4 High-rate discharge ability (A) for PGM-PPy film electrode (*a*) and GM-PPy film (*b*). The total "current on" time of PPy film is 40 s

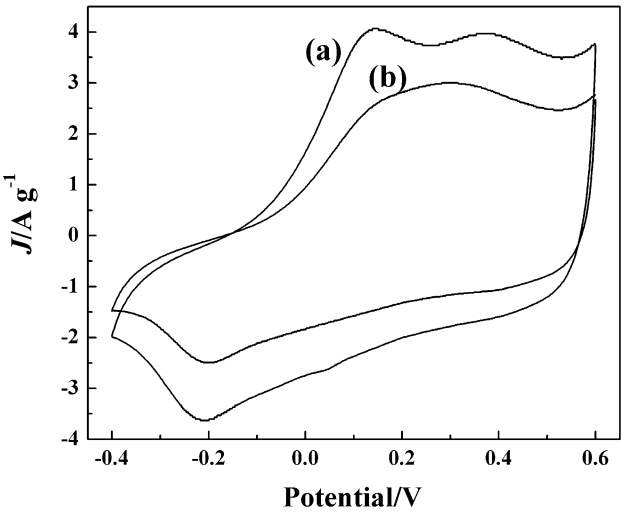

Fig. 5 CV curves of PGM-PPy film (*a*) and GM-PPy film (*b*) in1 M H_2SO_4 electrolyte at 5 mV s^{-1}

films by two polymerization method were similar as shown in Fig. 5. Both CV curves of PPy films in Fig. 5 shows a broad oxidation peak around −0.2 to 0.3 V. Both oxidation and reduction currents decrease toward the negative potential end, which is an indication of the polymer gradually becoming inactive and resistive. In the same potential range, the PGM-PPy film CV shows larger peak current compared with that of GM-PPy film, even at potentials close to the negative end. This difference in current between GM-PPy and PGM-PPy can be explained as the latter has a uniform microstructure with small particle size structure for ion transport and improvement of hydrophilicity. It was very important to study the electrochemical properties of electrode materials in the neutral medium, because it was well known that the electrode material was more applicable and extensively used for the application of supercapacitors in the neutral medium [18]. Figure 6 illustrates the CV curves of PGM-PPy film electrode measured in 1 M $NaNO_3$ electrolyte at a scan rate of 5 mV s^{-1}. From Fig. 6, important information could be noticed, the curve of PGM-PPy film in 1 M $NaNO_3$ electrolyte with respect to the zero-current line and a rapid current response on voltage reversal at each end potential, as well as the rectangular-like and almost symmetric *I–E* responses of ideal capacitive behavior, which match the requirement of the application as supercapacitors.

The above studies proposed that the PGM-PPy film electrode had a higher SC and better high-rate discharge ability, which led to good capacitance properties. Therefore, we carried out the following EIS investigation to prove the good capacitive performance of PGM-PPy film electrode.

Electrochemical impedance spectroscopy

From Fig. 7, we can see the impedance spectra of PGM-PPy film and GM-PPy film in 1 M H_2SO_4 electrolyte at

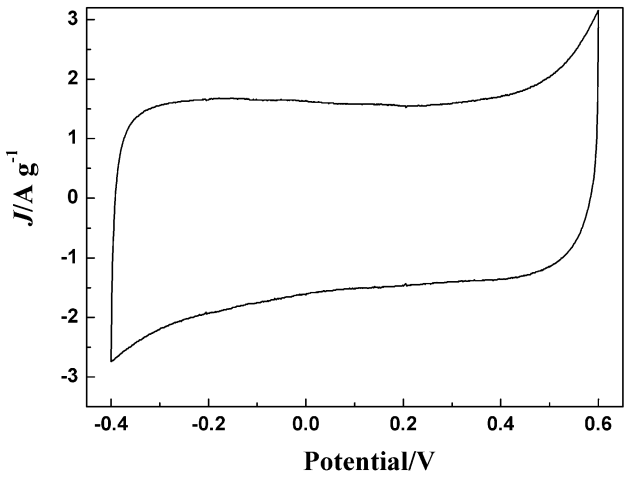

Fig. 6 CV curve of the PGM-PPy film (total "current on" time of 40 s) at a scan rate of 5 mV s^{-1} in 1 M $NaNO_3$ electrolyte

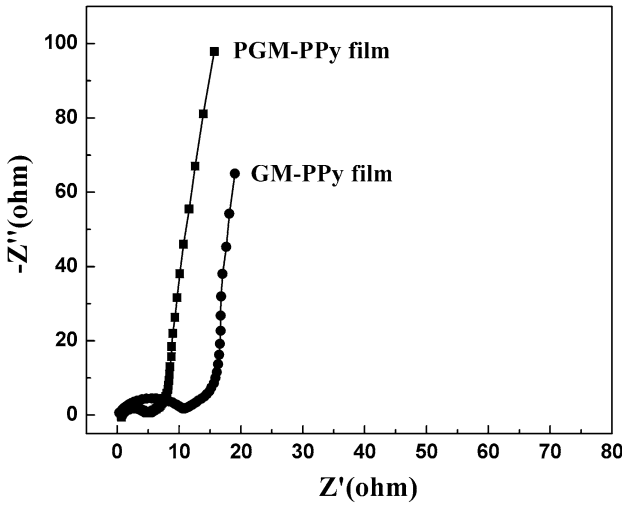

Fig. 7 Impedance Nyquist plots of the PGM-PPy film (*a*) and GM-PPy film (*b*) (0.32 V vs. SCE; electrolyte: 1 M H_2SO_4)

open circuit voltage (OCV). Both curves are similar in form, composed of a single semicircle in high-frequency and straight line in the low-frequency region. First, in high-frequency intercept of the real axis, an internal resistance (*R*s) can be observed, which included the resistance of the electrolyte, the intrinsic resistance of the active material, and the contact resistance at the interface active material/current collector. The value of *R*s for both PGM-PPy film electrode and GM-PPy film electrode was 0.7 Ω cm^{-2}. Second, as shown in Fig. 7, the electrochemical charge-transfer resistance (R_{ct}) (which was evaluated by the real part of the impedance between low and high frequencies [33, 34]) of PGM-PPy film electrode is smaller than GM-PPy film, which indicates that the PGM-PPy film electrode has smaller R_{ct} than that of GM-PPy film. This can be explained by the thickness and microstructure of the PPy film. With the same total "current on" time, the GM-PPy film is thicker than PGM-PPy film, which could be confirmed from the mass value in Table 1. The GM-PPy film shows a rough surface with large particle size and thickness, such a structure did not favor and enhance the diffusivity of the electrolyte ions into the film. Hence, the thinner PGM-PPy film with good hydrophilic character and smooth surface exhibits good capacitance behavior due to the smaller R_{ct}. Therefore, in low frequency, the diffusing line comes close to an ideal straight line along the imaginary axis without the obvious presence of 45° plot, which was characteristic feature of capacitive behavior.

The EIS curves of PGM-PPy film at OCV, 0.6 V (vs. SCE), and −0.4 V (vs. SCE) are shown in Fig. 8a. Two features should be noted for all three curves in Fig. 8a. The value of R_S is nearly invariant, keeping a value of 0.7 Ω cm^{-2} for all voltages of the PGM-PPy film

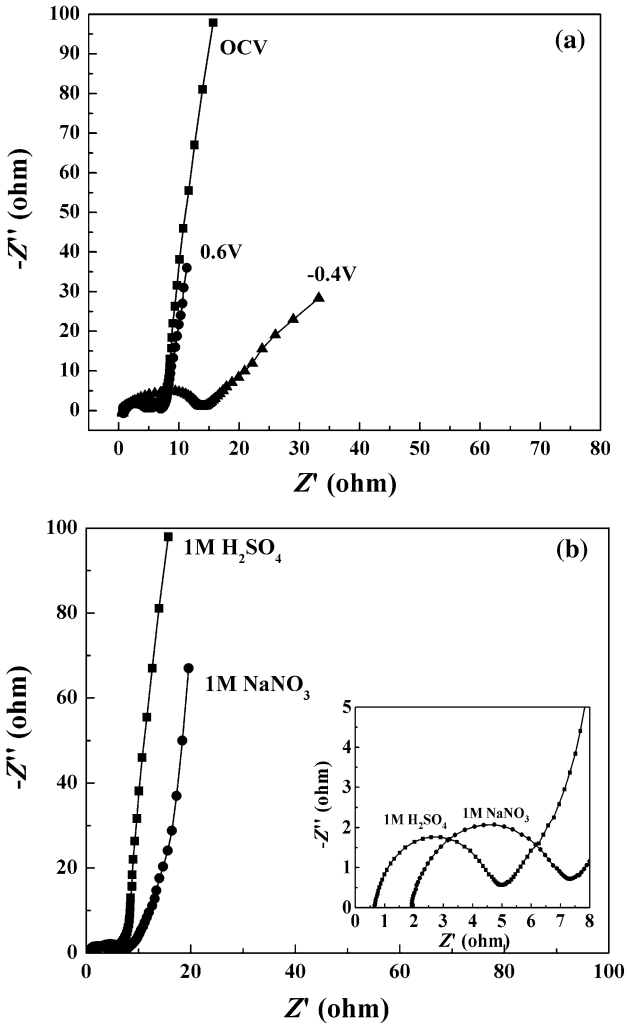

Fig. 8 Impedance Nyquist plots of PGM-PPy film: **a** measured at OCV (0.32 V), 0.6 V and −0.4 V in 1 M H_2SO_4 solution; **b** measured in 1 M H_2SO_4 electrolyte and 1 M $NaNO_3$ electrolyte

electrode. In Fig. 8a, the R_{ct} of the three curves are obviously different. The value of PPy film from Fig. 8a was about 4.2 Ω cm^{-2} at open circuit voltage (OCV), because of the high electronic conductivity and fast response ability of the PPy film. The value of R_{ct} increasing up to 6.3 Ω cm^{-2} at 0.6 V is due to the decrease of electrochemical activity of PPy resulting from an over oxidation beginning. Further increase would occur at −0.4 V, due to the reduced volume [35, 36] and the relatively lower electronic conductivity [37] of polymer at dedoped state. It could eventually reach 13.2 Ω cm^{-2}.

The typical EIS spectra of PGM-PPy film in 1 M H_2SO_4 electrolyte and 1 M $NaNO_3$ electrolyte are given in Fig. 8b, and there are two features between both curves. First, in high-frequency intercept of the real axis, a solution resistance *R*s can be observed. The value of PPy film was approximately 0.7 Ω cm^{-2} in 1 M H_2SO_4 electrolyte and 2.0 Ω cm^{-2} in 1 M $NaNO_3$. Second, in the medium-to-low frequency region, the unequal semicircular can be discovered from both curves. The radius of the semicircular in 1 M H_2SO_4 electrolyte was smaller than that in 1 M $NaNO_3$ electrolyte, the expanded portion is shown in the down-right corner of Fig. 8b. Herein, the charge-transfer resistance was smaller in the acidic electrolyte. In low frequency, the impedance plots were exhibited as a vertical line in 1 M H_2SO_4 electrolyte and a slightly tilted of vertical line in 1 M $NaNO_3$ electrolyte, both of which indicated a limiting diffusion process in two electrolytes and were the characteristic features of pure capacitive behavior [38].

Estimation of specific capacitance

The value of SC can be obtained from three techniques: cyclic voltammetry, galvanostatic charge–discharge, and impedance spectroscopy. As far as conducting polymers are concerned, the cyclic voltammetry with wide potential range includes the low doping (or undoped levels), so the polymer chains are not or less conjugated, and charge transfer occurs in a localized manner. Hence, at low doping levels it does not contribute to capacitance [39, 40]. At high doping levels (by shifting the potential positively), electrons are conjugated or delocalized along the polymer chain into conduction bands, which can contribute to the capacitance. Based on the analysis above, the CV is not suitable for capacitance measurements of PGM-PPy film in a wide potential range.

We calculated specific capacitances using galvanostatic charge–discharge techniques and impedance spectroscopy. The specific values were shown in Table 2. It is anticipated that both methods will not yield identical estimates in each case. Nevertheless, values deduced using galvanostatic charge–discharge experiments have more significance in view of their usefulness in fabrication of devices. On the other hand, impedance spectroscopy has the advantage of yielding not only specific capacitances but also other system parameters, such as double layer capacitance, charge transfer, ohmic and diffusional resistances.

Table 2 The SC of PGM-PPy film electrode obtained from different methods

Method	Formula	Specific capacitance (F g^{-1})
Galvanostatic charge–discharge	$C_d = I\Delta t/\Delta E\ m$	403 (0.5 mA cm^{-2})
		380 (1 mA cm^{-2})
		375 (3 mA cm^{-2})
		360 (5 mA cm^{-2})
Impedance spectroscopy	$*C_f = -1/(2\ m\pi f Z_{im})$	312 (OCV)

* C_f is the SC of the electrode; f is the frequency (0.01 Hz); Z_{im} is the imaginary part of the impedance test and m is the mass of the active materials

Conclusions

The PPy films were synthesized on SS electrode from aqueous solution containing 0.5 M TOS and 0.1 M pyrrole by pulse galvanostatic method. The process of PGM with short t_{on} (10 ms) and longer t_{off} (100 ms) resulted in a smooth, uniform, and small particle size of PPy film, which could be observed from SEM images. Such a structure favored ionic motion and hydrophilicity improvement. The supercapacitive behaviors of these films were investigated with cyclic voltammetry (CV), charge–discharge tests, and ac impedance spectroscopy. Compared with the GM-PPy film, the results revealed that with 40 s "current on" time the PGM-PPy film showed better capacitive characteristics and larger SC of 403 F g^{-1}. Moreover, the PGM-PPy film electrode exhibited better high-rate discharge ability, lower resistance, and more promise for applications in supercapacitor than GM-PPy film electrodes.

Acknowledgements This study was supported by the National Natural Science Foundation of China (No. 50602020) and the National Basic Research Program of China (No. 2007CB216408).

References

1. Skotheim TA, Elsenbaumer RL, Reynolds JR (1998) In: Dekker M (ed) Hand book of conducting polymers. New York
2. Boara G, Sparpaglione M (1995) Synth Met 72:135
3. Ryu KS, Kim KM, Park NG, Park YJ, Chang SH (2002) J Power Sources 103:305
4. Shchukin DG, Kohler K, Mohwald H (2006) J Am Chem Soc 128:4560

5. Zhou Q, Li CM, Li J, Cui X, Gervasio D (2007) J Phys Chem C 111:11216
6. Smit MA, Ocampo AL, Espinosa-Medina MA, Sebastián PJ (2003) J Power Sources 124:59
7. Ingram MD, Staesche H, Ryder KS (2004) J Power Sources 129:107
8. An KH, Jeon KK, Heo JK, Lim SC, Bae DJ, Lee YH (2002) J Electrochem Soc 149:A1058
9. Sabah S, Aghamohammadi M, Alizadeh N (2005) Sens Actuators B 114:489
10. Cosnier S, Ionescu RE, Herrmann S, Boufer L, Demeunynck M, Marks RS (2006) Anal Chem 78:7054
11. Goodwin JW, Markham GM, Vinent B (1997) J Phys Chem B 101:1961
12. Attarzadeh N, Raeissi K, Golozar MA (2008) Prog Org Coat 63:167
13. Lin XQ, Xu YH (2008) Electrochim Acta 53:4990
14. Xiao QF, Zhou X (2003) Electrochim Acta 48:575
15. Zhou CF, Kumar S (2005) Chem Mater 47:1997
16. Wang J, Xu YL, Chen X, Sun XF (2007) Compos Sci Technol 67:2981
17. Noh KA, Kim DW, Jin CS, Shin KH, Kim JH, Ko JM (2003) J Power Sources 124:593
18. Mi HY, Zhang XG, Ye XG, Yang SD (2008) J Power Sources 176:403
19. Hawkins SJ, Ratcliffe NM (2000) J Mater Chem 10:2057
20. Nakayama M, Yano J, Nakaoka K, Ogura K (2002) Synth Met 128:57
21. Kobayashi T, Yoneyama H, Tamura H (1984) J Electroanal Chem 161:419
22. Geetha S, Trivedi DC (2004) Mater Chem Phys 88:88
23. Schuhmann W, Kranz C, Wohlschlager H, Strohmeier J (1991) Biosens Bioelectron 12:1157
24. Tsakova V, Milchev A (1991) Electrochim Acta 36:1579
25. Zhou HH, Wen JB, Ning XH, Fu CP, Chen JH, Kuang YF (2007) Synth Met 157:98
26. Zhou HH, Jiao SQ, Chen JH, Wei WZ, Kuang YF (2004) Thin Solid Films 450:233
27. Sharma RK, Rastogi AC, Desu SB (2008) Electrochem Commun 10:268
28. Groenendaal L, Jonas F, Freitag D, Pielartzik H, Reynolds R (2000) Adv Mater 12:481
29. Wang J, Xu YL, Chen X, Du XF (2007) J Power Sources 163:1120
30. Kiani MS, Bhat NV, Davis FJ, Mitchell GR (1992) Polymer 33:4113
31. Belanger D, Ren X, Davey J, Uribe F, Gottesfeld S (2000) J Electrochem Soc 147:2923
32. Valaski R, Ayoubb S, Micaronib L, Hummelgena IA (2001) Thin Solid Films 388:171
33. Zhou YK, He BL, Zhou WJ, Li HL (2004) J Electrochem Soc 151:A1052
34. Kong LB, Zhang J, An JJ, Luo YC, Kang L (2008) J Mater Sci 43:3664. doi:10.1007/s10853-008-2586-1
35. Zhang J, Kong LB, Wang B, Luo YC, Kang L (2009) Synth Met 159:260
36. Otero TF, Boyano I (2003) J Phys Chem B 107:6730
37. Sutar D, Menon R (2002) Thin Solid Films 417:40
38. Frackowiak E, Delpeux S, Jurewicz K, Szostak K, Cazorla-Amoros D, Beguin F (2002) Chem Phys Lett 361:35
39. Ramya R, Sangaranarayanan MV (2008) J Chem Sci 120:25
40. Peng C, Jin J, Chen GZ (2007) Electrochim Acta 53:525